ELSEVIER

Contents lists available at ScienceDirect

Science Bulletin

journal homepage: www.elsevier.com/locate/scib



Article

A common origin of muon g-2 anomaly, Galaxy Center GeV excess and AMS-02 anti-proton excess in the NMSSM

Murat Abdughani ^a, Yi-Zhong Fan ^{a,b,*}, Lei Feng ^{a,b,c}, Yue-Lin Sming Tsai ^{a,*}, Lei Wu ^{d,*}, Qiang Yuan ^{a,b}

- ^a Key Laboratory of Dark Matter and Space Astronomy, Purple Mountain Observatory, Chinese Academy of Sciences, Nanjing 210023, China
- ^b School of Astronomy and Space Science, University of Science and Technology of China, Hefei 230026, China
- ^cJoint Center for Particle, Nuclear Physics and Cosmology, Nanjing University Purple Mountain Observatory, Nanjing 210093, China
- ^d Department of Physics and Institute of Theoretical Physics, Nanjing Normal University, Nanjing 210023, China

ARTICLE INFO

Article history: Received 13 July 2021 Received in revised form 14 July 2021 Accepted 15 July 2021 Available online 21 July 2021

Keywords:
Dark matter
Supersymmetry
Muon g-2 anomaly
Galactic center GeV excess
Anti-proton excess
Global analysis

ABSTRACT

The supersymmetric model is one of the most attractive extensions of the Standard Model of particle physics. In light of the most recently reported anomaly of the muon g-2 measurement by the FermiLab E989 experiment, and the excesses of gamma rays at the Galactic center observed by Fermi-LAT space telescope, as well as the antiproton excess observed by the Alpha Magnetic Spectrometer, we propose to account for all these anomalies or excesses in the Next-to-Minimal Supersymmetric Standard Model (NMSSM). Considering various experimental constraints including the Higgs mass, B-physics, collider data, dark matter relic density and direct detections, we find that a \sim 60 GeV bino-like neutralino is able to successfully explain all these observations. Our scenario can be sensitively probed by future direct detection experiments.

© 2021 Science China Press. Published by Elsevier B.V. and Science China Press. All rights reserved.

1. Introduction

The muon anomalous magnetic moment a_{μ} has been very recently measured by E989 at Fermilab with an unprecedentedly relative precision of 368 parts-per-billion (ppb). By combining the new data with the previous measurement from Brookhaven National Lab (BNL) [1], they found a deviation $\delta a_{\mu} = (2.51 \pm 0.59) \times 10^{-9}$ with 4.2σ significance [2] from the Standard Model (SM) prediction. This indeed calls for the new physics beyond the Standard Model (BSM) [3–9].

Meanwhile, various astrophysical and cosmological observations show that the dark matter (DM) constitutes the majority of matter in the universe. Among many DM candidates, the weakly interacting massive particles (WIMPs) have been a compelling candidate. The appeal of WIMP DM is due in part to the suggestive coincidence between the thermal abundance of WIMPs and the observed DM density through the thermal freeze-out mechanism, known as the WIMP miracle. There have been various experiments devoted in the quest of nature of DM. The indirect detections of DM from searching for the gamma rays and cosmic rays have reported

E-mail addresses: yzfan@pmo.ac.cn (Y.-Z. Fan), smingtsai@pmo.ac.cn (Y.-L.S. Tsai), leiwu@njnu.edu.cn (L. Wu).

some intriguing excesses. For examples, the Galaxy center GeV gamma-ray excess (GCE) from the Fermi LAT [10–15] and the possible anti-proton excess from AMS-02 collaborations [16–19], they can be consistently interpreted as the $\sim 50-100$ GeV DM annihilating into the $b\bar{b}$ final states.

In conjuncture with the muon g-2 anomaly, all these anomalies may indicate the new physics in dark sector. Supersymmetry (SUSY) naturally provides the DM candidate, such as the lightest neutralino for R-parity conserving scenario. In SUSY, the muon g-2 anomaly can be explained by the contributions of light electroweakinos and sleptons running in the loops [20-24]. Although the low mass neutralino in the CP-conserving Minimal Supersymmetric Standard Model is still favored by muon g-2 anomaly, it cannot interpret the GCE because of p-wave suppressed annihilation cross section [25]. On the other hand, a new CP-odd singlet in the Next-to-Minimal Supersymmetric Standard Model (NMSSM) can play the role of a mediator in DM annihilation [26]. Once the mass of this singlet Higgs is just as heavy as two neutralino masses (singlet Higgs resonance), neutralino can effectively s-wave annihilate to the $b\bar{b}$ final state at the zero temperature. Consequently, the parameter space allowed by muon g-2 measurement may coincide with the GCE and anti-proton excess.

In this paper, we first perform a state-of-art analysis and find out that the anomalous muon *g*-2, GCE and the anti-proton excess

^{*} Corresponding authors.

may have a common physical origin that relates with DM in the NMSSM. We then show that such a scenario can be effectively probed in the future DM direct detection (DD) experiments.

2. Model and methodology

In the scale invariant NMSSM [27], a Z_3 symmetric gauge singlet chiral superfield \hat{S} is introduced. In addition to MSSM, the superpotential is

$$W = W_{\rm MSSM} + \lambda S H_u H_d + \frac{\kappa}{3} S^3, \tag{1}$$

where the new singlet Higgs develops a vev $\langle S \rangle = s$. The superpartner of S (singlino) can mix with gaugino and Higgsino as the neutralino mass matrix

$$M_{\chi^{0}} = \begin{pmatrix} M_{1} & 0 & -m_{Z}c_{\beta}s_{W} & m_{Z}s_{\beta}s_{W} & 0 \\ & M_{2} & m_{Z}c_{\beta}c_{W} & -m_{Z}s_{\beta}c_{W} & 0 \\ & 0 & -\mu & -\lambda\nu_{u} \\ & & 0 & -\lambda\nu_{d} \\ & & & \frac{2\kappa}{2}\mu \end{pmatrix}.$$
 (2)

The 5×5 unitary matrix is defined in the group basis (Bino B^0 , Wino W^0 , Higgsino h_u , Higgsino h_d , Singlino s^0). The effective μ -term is defined by λs and the Z-boson mass is m_Z . The vacuum expectation values for h_u and h_d are denoted as v_u and v_d . Their ratio is $\tan \beta = v_u/v_d$ and we define $s_\beta = \sin \beta$ and $c_\beta = \cos \beta$. Similarly, the sine and cosine of Weinberg angle are s_W and c_W . The gaugino mass M_1 and M_2 are the soft bino and wino masses. After diagonalized, the lightest neutralino χ_1^0 can be DM by assuming R-parity conserved.

In this work, we narrow down the list of the NMSSM parameters to nine free inputs and their prior ranges are

$$\begin{split} &0.001 < \lambda < 1, 0.001 < |\kappa| < 2, |A_{\lambda}| < 3000, |A_{\kappa}| < 20, \\ &30\,\text{GeV} < M_1 < 80\,\text{GeV}, 100\,\text{GeV} < M_2 < 1000\,\text{GeV}, \\ &100\,\text{GeV} < |\mu| < 1000\,\text{GeV}, 100\,\text{GeV} < M_{\tilde{\ell}_{1,2}} < 1000\,\text{GeV}, 1 < \tan\beta < 60, \\ &(3) \end{split}$$

where the soft-breaking mass parameters of the electroweakinos and sleptons are chosen to be less than 1 TeV to produce a sizable positive corrections to the muon g-2 [28], while the small M_1 is required to produce the GCE spectra [12]. Since our studied observables are mainly sensitive to the electroweakinos and sleptons, other irrelevant SUSY parameters, i.e., $A_{u,d,b,t,\ell}$, M_3 , M_{Q_L} , M_{U_R} , M_{D_R} , M_{E_3} and M_{L_3} , are set to 3 TeV to be decoupled for simplicity. Note that one can set these parameters to other high mass scale but our conclusions are not changed.

In Table 1, we summarize the sets of experimental constraints that we invoke in the likelihood functions for the numerical scan.

Table 1The experimental constraints used in this study.

Category	Experimental observables
DM relic density	$\Omega_{\gamma}h^2 = \Omega h^2 = 0.1186 \pm 0.002 \pm 0.1 \mu_t$ [29]
B physics	BR($B \to X_s \gamma$) = $(3.27 \pm 0.14 \pm 0.1 \mu_t) \times 10^{-4}$ [30]
	$BR(\textit{B}_{s}^{0} \rightarrow \mu^{+}\mu^{-}) = (3.0 \pm 0.6 \pm 0.3) \times 10^{-9} \text{ [31]}$
	BR($B_u \to \tau \nu$) = $(1.09 \pm 0.24 \pm 0.1 \mu_t) \times 10^{-4}$ [32]
Higgs physics	$R_{ m inv} < 9\%$ at 95% CL [33]
	$m_{h_{\rm SM}} = (125.36 \pm 0.41 \pm 2.0) \; \; {\rm GeV} \; [34]$
DM DD	XENON1T [35,36], PICO-60 [37]
muon (g-2)	$\delta a_{\mu}^{old} = (2.61 \pm 0.48 \pm 0.63) \times 10^{-9} \ \text{[32]}$
	$\delta a_{\mu}^{\text{new}} = (2.51 \pm 0.59) \times 10^{-9} \text{ [2]}$
GCE	As implemented in Ref. [38]
LHC	$pp o \chi_1^+ \chi_1^-, \; pp o \chi_1^\pm \chi_2^0 \; ext{and} \; pp o ilde{\ell}_{LR}^+ ilde{\ell}_{LR}^$

We define the total $\chi^2_{\rm tot}$ is the sum of χ^2_i where i runs over all the constraints in Table 1. Beside the constraints (DM DD, GCE, and LHC), we use Gaussian likelihood for the rest constraints and their γ^2 is defined as

$$\chi^2 = \left(\frac{\mu_t - \mu_0}{\sigma}\right)^2 \text{ and } \sigma = \sqrt{\sigma_{theo}^2 + \sigma_{exp}^2}, \tag{4}$$

where μ_t is the theoretical prediction we calculated, μ_0 is the experimental central value and σ is the uncertainty including both theoretical and experimental errors.

We perform several random scans in the range as defined in Eq. (3). Except λ and κ are scan with log prior, the priors of the rest seven parameters are linear uniform distributed. We applied Metropolis–Hastings algorithm to undertake the focused scan at the parameter space with higher probability. The mass spectra and decay information are generated by using NMSSMTools-5.5.2 [39], and B-physics predictions are obtained by using SuperIso-4.0 [40]. We use package MicroMEGAs-5.2.6 [41] for the calculation of DM relic density, muon δa_{μ} , and DM-nucleon cross sections.

Regarding the LHC constraints, we also consider the exclusions from the null results of searching for the SUSY events with two or three leptons plus missing transverse momentum at the 13 TeV LHC with the luminosities of 36.1 [42] and 139 fb⁻¹ [43], respectively. We simulate the signal processes (i) $pp \to \chi_1^+ \chi_1^-$, (ii) $pp o \chi_1^\pm \chi_2^0$ and (iii) $pp o ilde{\ell}_{L,R}^+ ilde{\ell}_{L,R}^-$ are simulated by <code>MadGraph5_-</code> aMC-v3.1.0 [44] with default parton distribution function [45]. The next-to-leading order corrections to the cross sections of the above processes are included by using the factor K = 1.5. Then the parton-level events are showered and hadronized with PYTHIA-8.3 [46]. The detector effects are implemented by using DELPHES-3.4.1 [47]. The package CheckMATE-2.0.29 is used to recast the LHC analyses for each sample. Finally, we define the event ratio $r = \max(N_{s,i}/S_{obs,i}^{95\%})$ for each experimental analysis, where $N_{S,i}$ is the number of the events for the *i*-th signal region and $S^{95\%}$ is the corresponding observed 95% C.L. upper limit. The max is over all the signal regions for each analysis. As long as r > 1, we can conclude that such a sample is excluded at 95% confidence limit (CL).

3. Result

To demonstrate the impact of new δa_{μ} result and GCE signal on the NMSSM parameter space, we group the constraints except δa_{μ} , Fermi GCE, and LHC as basic set. Its statistic strength is denoted by $\chi^2(\text{basic})$. We can see the role of new δa_{μ} result by comparing the old and new δa_{μ} result and we define their relevant chi-squares as $\chi^2(\text{basic} + \delta a_{\mu}^{\text{old}})$ and $\chi^2(\text{basic} + \delta a_{\mu}^{\text{new}})$. Finally, the Fermi GCE data squeeze the parameter space to close to $m_{\chi} \approx 60$ GeV and cross section around $\langle \sigma v \rangle \approx 2 \times 10^{-26}$ cm³ s⁻¹. Our total chi-square including GCE data is $\chi^2(\text{basic} + \delta a_{\mu}^{\text{new}} + \text{GCE})$. We define the gray and green layers are $\delta \chi^2(\text{basic} + \delta a_{\mu}^{\text{new}}) < 5.99$ (gray points), $\delta \chi^2(\text{basic} + \delta a_{\mu}^{\text{new}}) < 5.99$ (green points), respectively. The top layer (red points) is with a slightly different definition. On top of the criteria $\delta \chi^2(\text{basic} + \delta a_{\mu}^{\text{new}}) < 5.99$, we further require the survival red points to agree with LHC and GCE data within 95% CL.

The propagator masses $m_{\chi_1^0}$, $m_{\chi_1^\pm}$, $m_{\widetilde{\mu}}$ and $m_{\widetilde{\nu}_{\mu}}$ enter the one-loop level of δa_{μ} computation. In Fig. 1, we show the correlation between the geometric average of these four masses and δa_{μ} . The shaded blue belt is the 1σ error bar of new g-2 data. We find that the geometric average of these four masses has an upper limit at

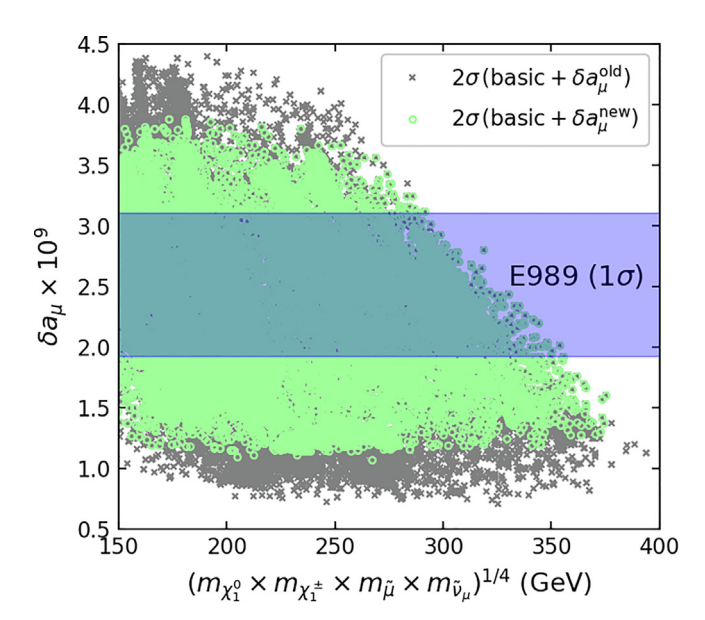


Fig. 1. The distribution of 2σ allowed samples. We predict the value of δa_{μ} with respect to the geometric mean of the masses of χ_1^0 , χ_1^\pm , $\tilde{\mu}$, and $\tilde{\nu}_{\mu}$. The grey (green) scatter points are 2σ allowed samples by basic $+\delta a_{\mu}^{\rm old\, new)}$ constraints. The shaded blue belt presents the E989 1σ region.

around 400 GeV by applying $\delta a_{\mu}^{\rm old}$ while the upper limit becomes 375 GeV when updating to $\delta a_{\mu}^{\rm new}$.

Since we are only interested in a lighter neutralino mass region, the contribution of the neutralino-smuon loop with a light DM is usually dominant. As a drawback, the correlation between neutralino and smuon does not clearly appear from δa_μ one-loop computation. We find from our scan that the production of mass scale $\sqrt{m_{\chi_1^\pm} m_{\bar{\nu}_\mu}}$ is pushed to be less than 600 GeV in 2σ after $\delta a_\mu^{\rm new}$ is applied. Note that the contribution of second chargino χ_2^\pm can also be as important as the one from χ_1^\pm if they are nearly degenerated.

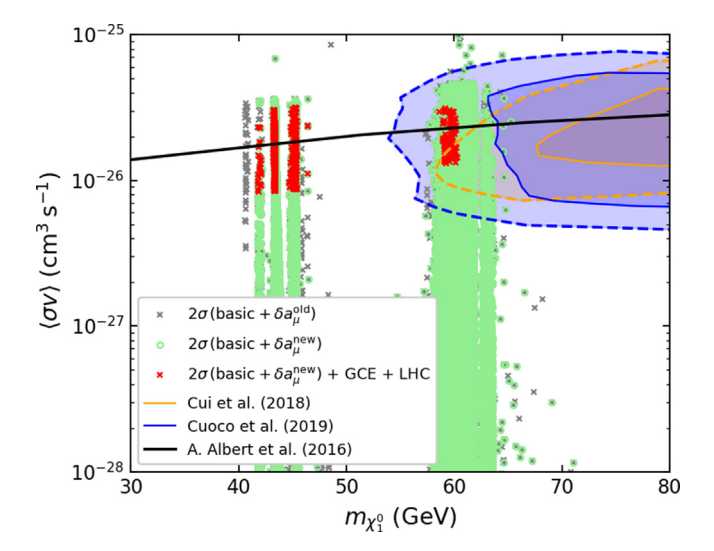


Fig. 2. The annihilation cross section $\langle \sigma v \rangle$ vs. $m_{\chi_1^0}$. The grey, green and red dots are defined as legend. The orange solid and dashed contours are for the anti-proton 68% and 95% C.L. from Ref. [48]. The blue solid and dashed contours are for the anti-proton 68% and 95% C.L. from Ref. [19]. Irrelevant region $\langle \sigma v \rangle < 10^{-28}$ cm³ s⁻¹ was truncated. In this work, we do not include the bound set by the dwarf spheroidal galaxy observations [49] (black solid line), because some recent investigations show that the previous researches likely have significantly overestimated the stringentness of the limits [50,51].

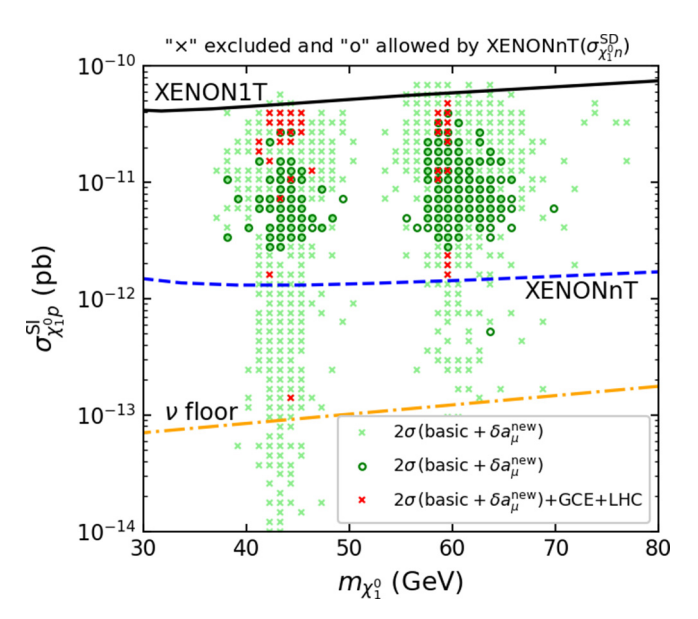


Fig. 3. The DM-proton spin-independent cross section vs. DM mass $m_{\chi_1^0}$. The dark and light green samples agree with χ^2 (basic + $\delta a_\mu^{\rm new}$) < 5.99. If the green samples pass the 95% limit of both GCE and LHC, they are presented by the red color. The black lines are XENON1T WIMP-proton SI [54] cross section 90% upper limits. The blue dashed lines are projected XENONNT [55] 90% upper limit which are similar to the future PandaX-4T sensitivities [56]. The dot-dashed orange line is the neutrino floor. The allowed samples by XENONNT $\sigma_{\chi n}^{\rm SD}$ limit are marked by "ο" while those excluded samples are marked by "×".

In Fig. 2, we project all the samples of three groups on the $(m_{\chi_1^0}, \langle \sigma v \rangle)$ plane. It is clear that the allowed DM mass are around either near Z-resonance $(m_\chi \simeq 45 \text{ GeV})$ or SM Higgs H resonance $(m_\chi \simeq 60 \text{ GeV})$ in order to fulfill the relic density constraints. If anti-proton excess is also included, only the samples near 60 GeV survived. Therefore, we conclude that the bino-like DM in the NMSSM may be the common origin of muon g-2 anomaly, GCE and AMS-02 anti-proton excess.

We would like to comment the possible constraints of the survived region near 60 GeV. Although the distortion of cosmic microwave background (CMB) power spectrum may be severe to DM annihilation to the leptonic final state, the CMB limits [52] cannot exclude the survived region where $b\bar{b}$ dominate the annihilation (more than 90% of total contribution). We found the subdominant channel is $\chi\chi\to\tau^+\tau^-$ which only contributes at most 10% in total. On the other hand, for $b\bar{b}$ final state annihilation, the Fermi gamma ray observations from dwarf spheroidal galaxies (dSphs) [53] can set a stronger bound than the one from CMB. In this work, we do not include the Fermi dSphs limit [49] but only present it in Fig. 2, because some recent investigations show that the previous researches likely have significantly overestimated the stringentness of the limits [50,51].

To match the observed relic density, DM annihilation cross section in the early universe is around $10^{-26}~{\rm cm^3~s^{-1}}$. In our work, this can be achieved through SM-Higgs h or Z gauge boson resonance annihilation. Because the pure bino does not couple with h or Z, the bino-like neutralino must contain some small fraction of higgsino ingredients in order to maintain h or Z resonance. If bino-like neutralino mass is not near the resonant area ~ 45 or ~ 60 GeV, it would require a large composition of higgsino to reduce the relic density. However, we find that the current XENON1T data restricts the higgsino composition up to $\sim 2\%$.

Nevertheless, DM momentum in the present universe is no longer to maintain a large cross section via the h and Z resonance.

Therefore, a new funnel is needed to undertake a cross section around $2\times 10^{-26}~{\rm cm^3~s^{-1}}$ for GCE. Unlike *CP*-conserving MSSM whose DM annihilation is *p*-wave suppressed at present, the pseudo-scalar mediator A_1 in the singlet sector of NMSSM can generate the *s*-wave process at zero temperature. One has to bear in mind that those annihilations in the present universe are via A_1 -resonance even if it can be *Z*-resonance or *H*-resonance in the early universe. The final state of the A_1 funnel annihilation is governed by the $b\bar{b}$ channel with more than 90% of total contribution. The subdominant annihilation final state is $\tau^+\tau^-$ and it contributes at most 10% in total.

In Fig. 3, we plot the spin-independent (SI) component of the DM-proton elastic scattering cross sections in function of $m_{\chi_1^0}$. The black lines represent 90% C.L. upper limits from XENON1T experiment [36,54]. There are some samples near the v floor, namely the blind spot region [57]. Although $\sigma_{\chi p}^{\rm SI}$ in the blind spot region is very small and even unreachable below the neutrino floor, one can still probe them by future WIMP-neutron spin-dependent (SD) cross section $\sigma_{\chi p}^{\rm SD}$ measurement as pointed out in Ref. [58]. We plot those samples allowed by XENONnT $\sigma_{\chi p}^{\rm SD}$ limit [55] with " \circ ", but those samples with $\sigma_{\chi p}^{\rm SD}$ larger than XENONnT sensitivity are "×"s. Indeed, the future XENONnT $\sigma_{\chi p}^{\rm SD}$ sensitivity can probe those small $\sigma_{\chi p}^{\rm SI}$. Eventually, the parameter space favored by GCE can be completely probed by future XENONnT underground detector.

Finally, we find that the current LHC SUSY particle searches are not able to completely exclude the region where all the excesses can be spontaneously explained. By scrutinizing the allowed charged particle masses with several 13 TeV LHC analyses, we obtain the approximate upper limits $m_{\tilde{\chi}_1^\pm} \gtrsim 300 \text{ GeV}$ and $m_{\tilde{u}} \gtrsim 500 \text{ GeV}$.

4. Conclusion

In this paper, we identify a common parameter space which can accommodate the muon g-2 anomaly, the GCE, and the anti-proton excess in the NMSSM. Considering various experimental constraints, e.g., the Higgs mass, B-physics, LHC data, DM relic density from PLANCK, and DM DDs, we find that the light eletroweakinos and sleptons with masses being lighter than about 1 TeV are required. The geometric average of their masses should be less than about 375 GeV to explain the muon g-2 anomaly. Only the bino-like neutralino DM can explain both the muon g-2 and the GCE. They need to resonantly annihilate through Z bosons or Higgs bosons to produce the correct relic density. On the other hand, in order to give enough DM annihilation cross section for the GCE, we need a singlet-like Higgs boson as the mediator in the schannel resonance process at present. When further including the anti-proton excess, we find that only the Higgs funnel is feasible. The favored parameter space of the NMSSM model discussed in this work can be critically probed by the future XENONnT underground detector. We also expect that such a parameter space can be covered by the future AMS-02 as long as anti-deuteron or anti-Helium could be detected [59].

Conflict of interest

The authors declare that they have no conflict of interest.

Acknowledgments

This work was supported by the National Natural Science Foundation of China (U1738210, 12047560, and 11773075), China Post-

doctoral Science Foundation (2020M681757), Chinese Academy of Sciences, and the Program for Innovative Talents and Entrepreneur in Jiangsu.

Author contributions

Yi-Zhong Fan conceived the idea. He also initiated this study with Lei Feng and Murat Abdughani. Murat Abdughani and Yue-Lin Sming Tsai conducted the numerical calculations, analyzed the physical results, and drafted major part of the manuscript. Lei Wu cross-checked the collider results and constraints. Yi-Zhong Fan, Lei Wu and Qiang Yuan wrote part of the manuscript. All authors discussed the results and revised the manuscript.

References

- Particle Data Group, Tanabashi M, et al. Review of particle physics. Phys Rev D 2018;98:030001.
- [2] Muon g-2 Collabration, Abi B, et al. Measurement of the positive muon anomalous magnetic moment to 0.46 ppm. Phys Rev Lett 2021;126:141801.
- [3] Aoyama T, Asmussen N, Benayoun M, et al. The anomalous magnetic moment of the muon in the Standard Model. Phys Rep 2020;887:1–166.
- [4] Das A, Nomura T, Okada H, et al. Generation of a radiative neutrino mass in the linear seesaw framework, charged lepton flavor violation, and dark matter. Phys Rev D 2017;96:075001.
- [5] Jana S, Vishnu PK, Saad S. Resolving electron and muon g-2 within the 2HDM. Phys Rev D 2020;101:115037.
- [6] Jana S, Vishnu PK, Rodejohann W, et al. Dark matter assisted lepton anomalous magnetic moments and neutrino masses. Phys Rev D 2020;102:075003.
- [7] Okada N, Tran HM. 125 GeV higgs boson mass and muon g-2 in 5D MSSM. Phys Rev D 2016;94:075016.
- [8] Endo M, Yin W. Explaining electron and muon g-2 anomaly in SUSY without lepton-flavor mixings. J High Energy Phys 2019;08:122.
- [9] Yin W, Yamaguchi M. Muon g-2 at multi-TeV muon collider. arXiv:2012.03928, 2020
- [10] Hooper D, Goodenough L. Dark matter annihilation in the galactic center as seen by the Fermi gamma ray space telescope. Phys Lett B 2011;697:412–28.
- [11] Zhou B, Liang Y-F, Huang X, et al. GeV excess in the Milky Way: the role of diffuse galactic gamma-ray emission templates. Phys Rev D 2015;91:123010
- diffuse galactic gamma-ray emission templates. Phys Rev D 2015;91:123010.

 [12] Calore F, Cholis I, Weniger C. Background model systematics for the Fermi GeV excess. J Cosmol Astropart Phys 2015;03:038.
- [13] Huang X, Enßlin T, Selig M. Galactic dark matter search via phenomenological astrophysics modeling. J Cosmol Astropart Phys 2016;04:030.
- [14] Fermi-LAT Collaboration, Ackermann M, et al. The Fermi galactic center GeV excess and implications for dark matter. Astrophys J 2017;840:43.
- [15] Hoof S, Geringer-Sameth A, Trotta R. A global analysis of dark matter signals from 27 dwarf spheroidal galaxies using 11 Years of Fermi-LAT observations. J Cosmol Astropart Phys 2020;02:012.
- [16] Cui M-Y, Yuan Q, Tsai Y-LS, et al. Possible dark matter annihilation signal in the AMS-02 antiproton data. Phys Rev Lett 2017;118:191101.
- [17] Cuoco A, Krämer M, Korsmeier M. Novel dark matter constraints from antiprotons in light of AMS-02. Phys Rev Lett 2017;118:191102.
- [18] Cholis I, Linden T, Hooper D. A robust excess in the cosmic-ray antiproton spectrum: implications for annihilating dark matter. Phys Rev D 2019;99:103026.
- [19] Cuoco A, Heisig J, Klamt L, et al. Scrutinizing the evidence for dark matter in cosmic-ray antiprotons. Phys Rev D 2019;99:103014.
- [20] Moroi T. The muon anomalous magnetic dipole moment in the minimal supersymmetric standard model. Phys Rev D 1996;53:6565–75.
- [21] Fowlie A, Kowalska K, Roszkowski L, et al. Dark matter and collider signatures of the MSSM. Phys Rev D 2013;88:055012.
- [22] Abe N, Endo M. Recent muon g-2 result in deflected anomaly mediated supersymmetry breaking. Phys Lett B 2003;564:73–82.
- [23] Czarnecki A, Marciano WJ. The muon anomalous magnetic moment: a Harbinger for "new physics". Phys Rev D 2001;64:013014.
- [24] Abdughani M, Hikasa K-I, Lei W, et al. Testing electroweak SUSY for muon g-2 and dark matter at the LHC and beyond. J High Energy Phys 2019;11:095.
- [25] Carena M, Osborne J, Shah NR, et al. Return of the WIMP: missing energy signals and the galactic center excess. Phys Rev D 2019;100:055002.
- [26] Kowalska K, Munir S, Roszkowski L, et al. Constrained next-to-minimal supersymmetric standard model with a 126 GeV Higgs boson: a global analysis. Phys Rev D 2013;87:115010.
- [27] Konig H. Influence of the minimal supersymmetric standard model extended by an additional Higgs singlet on the anomalous magnetic moment of the muon. Z Phys C 1991;52:159–64.
- [28] Domingo F, Ellwanger U. Constraints from the muon *g*-2 on the parameter space of the NMSSM. J High Energy Phys 2008;07:079.
- [29] Plank Collaboration, Ade P AR, et al. Planck 2015 results. XIII. cosmological parameters. Astron Astrophys 2016;594:A13.

[30] GAMBIT Flavour Workgroup, Bernlochner F U, et al. FlavBit: a GAMBIT module for computing flavour observables and likelihoods. Eur Phys J C 2017;77:786.

- [31] LHCb Collaboration, Aaij R, et al. Measurement of the $B_s^0 \to \mu^+\mu^-$ branching fraction and effective lifetime and search for $B^0 \to \mu^+\mu^-$ decays. Phys Rev Lett 2017:118:191801.
- [32] Particle Data Group, Zyla PA, et al. Review of particle physics. Prog Theor Exp Phys 2020;8:083C01.
- [33] ATLAS Collaboration, Aad G, et al. A combination of measurements of Higgs boson production and decay using up to 139 fb⁻¹ of proton–proton collision data at √s = 13 TeV collected with the ATLAS experiment. ATLAS-CONF-2020-027.
- [34] Bechtle P, Heinemeyer S, Stal O, et al. Applying exclusion likelihoods from LHC searches to extended higgs sectors. Eur Phys J C 2015;75:421.
- [35] XENON Collaboration, Aprile E, et al. Dark matter search results from a one ton-year exposure of XENON1T. Phys Rev Lett 2018;121:111302.
- [36] XENON Collaboration, Aprile E, et al. Constraining the spin-dependent WIMPnucleon cross sections with XENON1T. Phys Rev Lett 2019;122:141301.
- [37] PICO Collaboration, Amole C, et al. Dark matter search results from the complete exposure of the PICO-60 C₃F₈ bubble chamber. Phys Rev D 2019:100:022001.
- [38] Calore F, Cholis I, McCabe C, et al. A tale of tails: dark matter interpretations of the Fermi GeV excess in light of background model systematics. Phys Rev D 2015;91:063003.
- [39] Ellwanger U, Hugonie C. NMHDECAY 2.0: an updated program for sparticle masses, Higgs masses, couplings and decay widths in the NMSSM. Comput Phys Commun 2006;175:290–303.
- [40] Mahmoudi F. Superlso v2.3: a program for calculating flavor physics observables in Supersymmetry. Comput Phys Commun 2009;180:1579–613.
- [41] Belanger G, Boudjema F, Brun P, et al. Indirect search for dark matter with micrOMEGAs2.4. Comput Phys Commun 2011;182:842–56.
- [42] ATLAS Collaboration, Aaboud M, et al. Search for electroweak production of supersymmetric particles in final states with two or three leptons at $\sqrt{s}=13$, TeV with the ATLAS detector. Eur Phys J C 2018;78:995.
- [43] ATLAS Collaboration, Aad G, et al. Search for electroweak production of charginos and sleptons decaying into final states with two leptons and missing transverse momentum in $\sqrt{s} = 13$ TeV pp collisions using the ATLAS detector. Eur Phys | C 2020;80:123.
- [44] Alwall J, Frederix R, Frixione S, et al. The automated computation of tree-level and next-to-leading order differential cross sections, and their matching to parton shower simulations. J High Energy Phys 2014;07:079.
- [45] Buckley A, Ferrando J, Lloyd S, et al. LHAPDF6: parton density access in the LHC precision era. Eur Phys J C 2015;75:132.
- [46] Sjöstrand T, Ask S, Christiansen JR, et al. An introduction to PYTHIA 8.2. Comput Phys Commun 2015;191:159–77.
- [47] DELPHES 3 Collabration, de Favereau J, et al. DELPHES 3, a modular framework for fast simulation of a generic collider experiment. J High Energy Phys 2014:02:057.
- [48] Cui M-Y, Pan X, Yuan Q, et al. Revisit of cosmic ray antiprotons from dark matter annihilation with updated constraints on the background model from AMS-02 and collider data. J Cosmol Astropart Phys 2018;06:024.
- [49] Fermi-LAT and DES Collaborations, Albert A, et al. Searching for dark matter annihilation in recently discovered milky way satellites with Fermi-LAT. Astrophys J 2017;834:110.
- [50] Ando S, Geringer-Sameth A, Hiroshima N, et al. Structure formation models weaken limits on WIMP dark matter from dwarf spheroidal galaxies. Phys Rev D 2020:102:061302.
- [51] Grand RJJ, White SDM. Baryonic effects on the detectability of annihilation radiation from dark matter subhaloes around the Milky Way. Mon Not Roy Astron Soc 2021:501:3558–67.
- [52] Slatyer TR. Indirect dark matter signatures in the cosmic dark ages. I. Generalizing the bound on s-wave dark matter annihilation from Planck results. Phys Rev D 2016;93:023527.
- [53] Fermi-LAT and DES Collabrations, Albert A, et al. Searching for dark matter annihilation in recently discovered Milky Way satellites with Fermi-LAT. Astrophys J 2017:834:110.
- [54] XENON Collabration, Gangi PD, et al. Results of the 1 tonne \times year WIMP search with XENON1T. Nuovo Cim C 2019;42:76.
- [55] XENON Collaboration, Aprile E, et al. Projected WIMP sensitivity of the XENONnT dark matter experiment. J Cosmol Astropart Phys 2020;11:031.
- [56] PandaX Collaboration, Zhang H, et al. Dark matter direct search sensitivity of the PandaX-4T experiment. Sci China Phys Mech Astron 2019;62:31011.
- [57] Abdughani M, Wu L, Yang J-M. Status and prospects of light bino-higgsino dark matter in natural SUSY. Eur Phys J C 2018;78:4.

- [58] Banerjee S, Matsumoto S, Mukaida K, et al. WIMP dark matter in a well-tempered regime: a case study on singlet-doublets fermionic WIMP. J High Energy Phys 2016;11:070.
- [59] Cholis I, Linden T, Hooper D. Antideuterons and antihelium nuclei from annihilating dark matter. Phys Rev D 2020;102:103019.



Murat Abdughani is a post-doctoral fellow at Purple Mountain Observatory, Chinese Academy of Sciences. His research interest mainly focuses on the dark matter, supersymmetry, collider phenomenology and machine learning.



Yi-Zhong Fan is a research professor and the director of the division of Dark Matter and Space Astronomy of Purple Mountain Observatory, Chinese Academy of Sciences. His research team, consisting of several groups, has very broad research interests, including dark matter indirect detection, gravitational wave astrophysics, high energy astrophysics, and space astronomy.



Yue-Lin Sming Tsai is an associate researcher at Purple Mountain Observatory, Chinese Academy of Sciences. He has been working on a wide range of complementary topics in the dark matter physics, including particle physics, astrophysics, cosmology, and statistics. In the past years, he and his collaborators conducted several global analyses to study dark matter phenomenology from a dark matter Lagrangian and experimental data sets.



Lei Wu is a professor at Nanjing Normal University. His research focuses on New Physics beyond the Standard Model, including dark matter, supersymmetry, collider physics and machine learning.